

Anisotropy of the Critical Current Density in Epitaxial  $\text{YBa}_2\text{Cu}_3\text{O}_x$  FilmsB. Roas<sup>(a)</sup> and L. Schultz*Siemens AG, Forschungslaboratorien, Postfach 3220, 8520 Erlangen, West Germany*

G. Saemann-Ischenko

*Physikalisches Institut, Universität Erlangen, Erwin Rommel Strasse 1, 8520 Erlangen, West Germany*

(Received 4 October 1989)

The critical current density  $j_c(B, T, \theta)$  of epitaxial,  $c$ -axis-oriented  $\text{YBa}_2\text{Cu}_3\text{O}_x$  films was measured between 4.2 and 77 K in magnetic fields up to 8 T as a function of the field direction  $\theta$ . Strongly enhanced critical currents are observed when the flux lines are aligned along the  $\text{CuO}$  planes, but there is also a maximum in  $j_c$  when the magnetic field is adjusted parallel to the  $c$  axis. We relate these effects to an intrinsic pinning between  $\text{CuO}$  layers, an anisotropy of the shear modulus  $c_{66}$ , and pinning effects of twin boundaries or stacking faults perpendicular to the film plane, respectively.

PACS numbers: 74.60.Jg, 74.60.Ge, 74.75.+t

Ceramic superconductors are well known to show a strong anisotropy in resistivity, critical current, and upper critical field  $B_{c2}$ .<sup>1</sup> A single-crystalline material is required to study the anisotropic behavior of the superconducting properties in detail. In this work the critical current density  $j_c$  in epitaxial,  $c$ -axis-oriented films is investigated as a function of the magnetic field direction up to 8 T for various temperatures.

The samples were prepared by laser deposition in an *in situ* process using a Siemens XP 2020 excimer laser (XeCl, 308 nm).<sup>2</sup> Epitaxial growth and  $c$ -axis orientation were achieved by heating the  $\langle 100 \rangle$   $\text{SrTiO}_3$  substrates to about 800°C and applying a 0.4-mbar oxygen atmosphere during the deposition. The 200- to 250-nm-thick films were patterned to 10- $\mu\text{m}$ -wide and 180- $\mu\text{m}$ -long strip lines using photoresist and wet-etching techniques.<sup>3</sup> The strip lines were randomly oriented with respect to the  $a$ - and  $b$ -axis directions in the  $\text{YBa}_2\text{Cu}_3\text{O}_x$  films. Silver was evaporated as a contact material after sputtering the film surface for 40 sec with Ar ions. The contacts had to withstand currents of more than 1 A passing the strip line at 4.2 K and corresponding to  $j_c$ 's up to  $5 \times 10^7 \text{ A/cm}^2$ .  $j_c$ , always measured perpendicular

to the magnetic field direction for all angles  $\theta$ , was determined by the four-probe technique with a voltage criterion of 0.5  $\mu\text{V}$ . The films were oriented with respect to the magnetic field direction from 0° to 180° as shown in Fig. 1(a). The current was reversed to simulate the range from 180° to 360°. The  $T_c$  ( $R=0$ ) of the film whose  $j_c$  values are presented in this work was 89.1 K, the resistivity was 76  $\mu\Omega \text{ cm}$  at 100 K and 242  $\mu\Omega \text{ cm}$  at 300 K.

The typical  $j_c(B)$  behavior for  $\mathbf{B} \perp \mathbf{c}$  and  $\mathbf{B} \parallel \mathbf{c}$  is plotted in Fig. 2. At  $T \leq 60 \text{ K}$  a maximum of the critical current density is obtained when the magnetic field is aligned along the film plane. However, at 77 K and  $B < 2 \text{ T}$  we observe higher  $j_c$  values when  $\mathbf{B}$  is perpendicular and parallel to the film plane. There is a crossover of the  $j_c(B)$  curves perpendicular and parallel to the film plane.  $j_c(\mathbf{B} \parallel \mathbf{c})$  drops to zero because the related  $B_{c2}$  is only about 6 T at this temperature. The crossover behavior is more pronounced for films grown at higher deposition rates [about 2  $\text{\AA}/(\text{laser pulse})$ ] and seems to

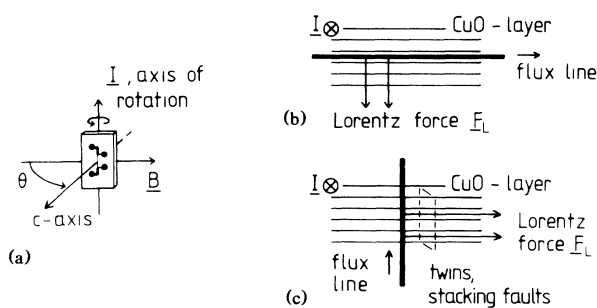


FIG. 1. (a) Directions of current, magnetic field, and film normal and definition of the tilt angle  $\theta$ . (b) Direction of the Lorentz force in the  $\mathbf{B} \perp \mathbf{c}$  case. (c) Direction of the Lorentz force in the  $\mathbf{B} \parallel \mathbf{c}$  case.

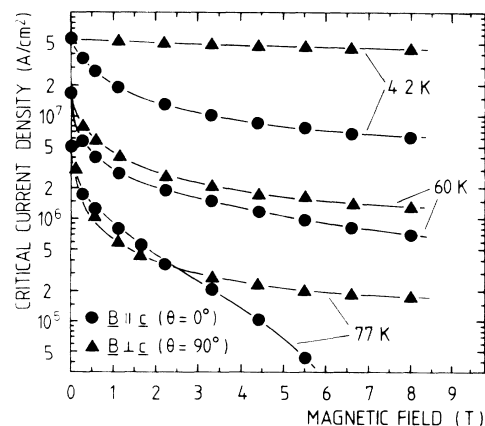


FIG. 2. Critical current density with  $\mathbf{B} \perp \mathbf{c}$  and  $\mathbf{B} \parallel \mathbf{c}$  at various temperatures in magnetic fields up to 8 T.

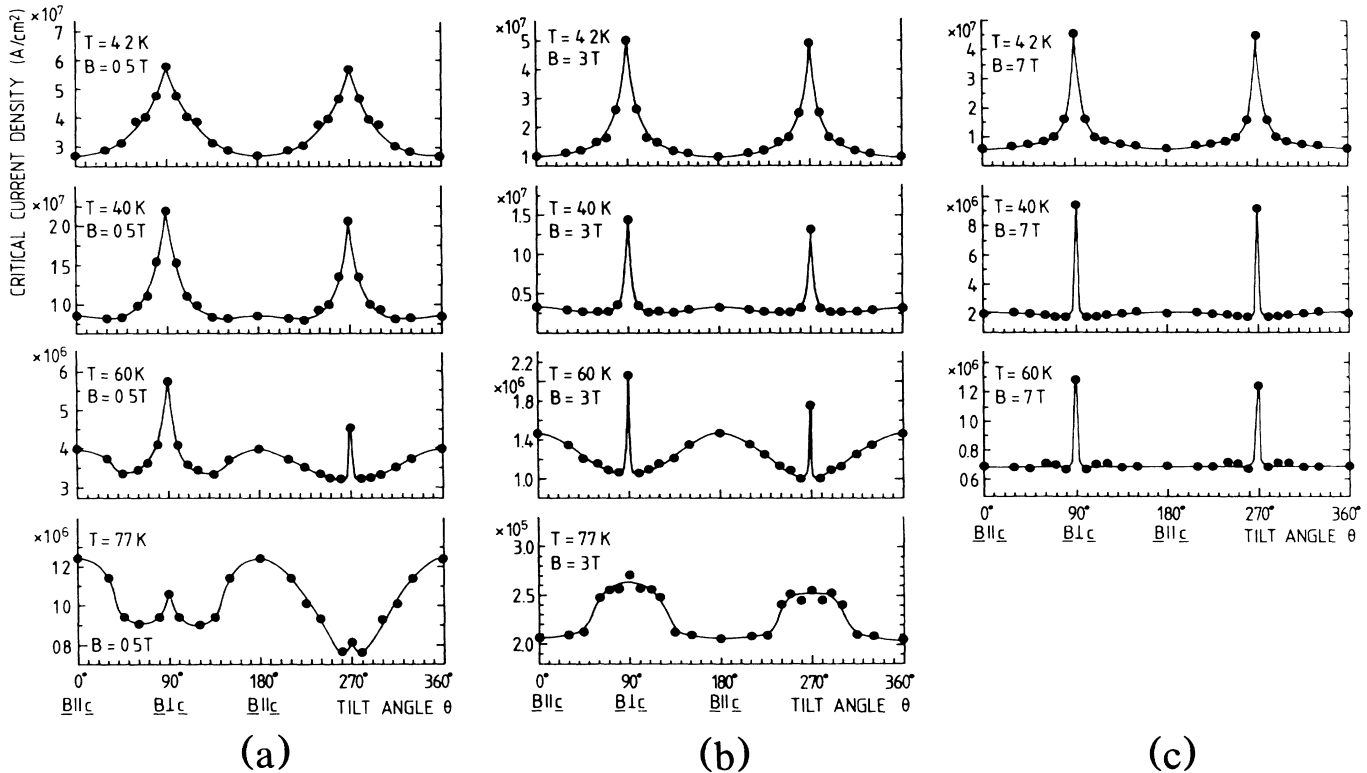


FIG. 3. Critical current density at different temperatures as a function of the angle  $\theta$  between  $\mathbf{B}$  and the film normal. Note the different  $j_c$  scaling for every plot: (a)  $B = 0.5 \text{ T}$ ; (b)  $B = 3 \text{ T}$ ; (c)  $B = 7 \text{ T}$ .

depend on microstructural features of the samples, as defect concentration, twin-boundary distance, etc. The  $j_c(B, T, \theta)$  behavior is given in detail in Fig. 3: (i) Extremely high  $j_c$  values are observed when the magnetic field is aligned parallel to the  $\text{CuO}$  planes ( $\mathbf{B} \perp \mathbf{c}$ ).  $j_c$  peaks can be seen at  $90^\circ$  and  $270^\circ$ ; at elevated temperatures those peaks are partly asymmetric. Slightly higher  $j_c$  values are obtained if the Lorentz force  $\mathbf{F} = \mathbf{j}_c \times \mathbf{B}$  is pointing to the film substrate interface [see Fig. 1(b)]. (ii) The  $j_c(\theta)$  function becomes more anisotropic with increasing  $B$ ; the peaks become narrower but less intense for increasing  $T$ . (iii) At 60 and 77 K, a relatively broad  $j_c$  maximum appears in the  $\mathbf{B} \parallel \mathbf{c}$  case.

For  $\mathbf{B} \perp \mathbf{c}$  the flux lines are parallel to the  $\text{CuO}$  planes and are driven across these planes by the Lorentz force towards the film-substrate interface or the film surface [depending on the current direction; see Fig. 1(b)]. Two mechanisms might be responsible for the strong pinning in the  $\mathbf{B} \perp \mathbf{c}$  case. One is an intrinsic pinning between the superconducting  $\text{CuO}$  planes,<sup>4,5</sup> assuming a modulation of the order parameter along the  $c$ -axis direction. The  $\text{CuO}$ -plane distance is comparable to the coherence length  $\xi_c$ . The maximal pinning is given if the flux lines are aligned exactly parallel to the film plane, thus interacting with the weakly superconducting layers between the  $\text{CuO}$  planes along the whole flux-line length. When the flux-line direction deviates by only a few de-

grees, they intersect these planes only at discrete points. The second effect is the anisotropy of the shear modulus  $c_{66}$  of the flux-line lattice in the 1:2:3 material, as discussed by Kogan and Campbell,<sup>6</sup> which is especially important at higher magnetic fields, where the interaction between the flux lines is enhanced. Kogan and Campbell calculated an easy motion of interacting flux lines along the planes and a large shear modulus, equivalent to a hindered flux-line motion across the planes. The stronger interaction between flux lines (weakly pinned flux lines can be held by the surrounding flux-line lattice) and especially the anisotropic properties of the flux-line lattice might explain the extremely high  $j_c$  values at 7 T. An additional pinning effect of the film interfaces<sup>7</sup> (surface and film-substrate interface) might be the reason the different  $j_c$  peak values at  $\theta = 90^\circ$  and  $270^\circ$ , which are observed for  $T = 60$  and  $77 \text{ K}$ . The different quality (roughness, strain) of the film surface and the film-substrate interface results in a differing shape of their pinning potential. Thus, different  $j_c$  values are expected when the Lorentz force is directed parallel or antiparallel to the film normal. We assume that it is not the rough film surface (a typical problem of the laser deposition process) but the film-substrate interface, with a lot of strain caused by the lattice mismatch, that affects the interface pinning. For increasing temperature the  $\mathbf{B} \perp \mathbf{c}$  pinning seems to be very weak. Con-

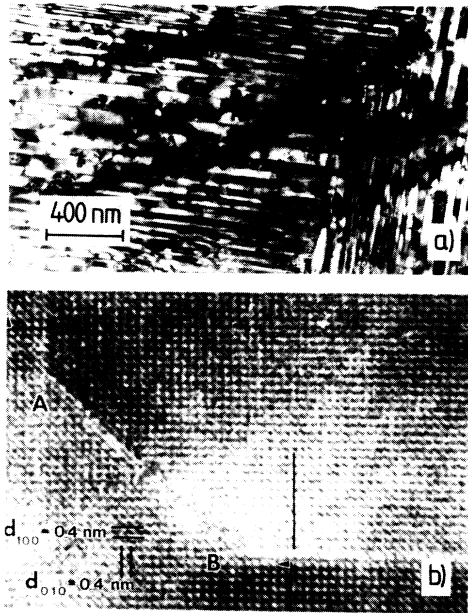


FIG. 4. (a) Twin boundaries along the [110] direction in a laser-deposited  $\text{YBa}_2\text{Cu}_3\text{O}_x$  film. The distance of two boundaries varies from 40 to 80 nm. (b) High-resolution transmission electron micrograph of an epitaxial film in the [001] pole. A stacking fault and a shift of the lattice by half of a unit cell can be seen.

sequently, there is only a relatively small  $j_c$  increase for  $\theta = 90^\circ$  or  $270^\circ$ . The weak pinning potential cannot hold the flux lines if they are not exactly aligned along the planes and therefore the  $j_c$  peak is very sharp. It should be mentioned that the penetration depth  $\lambda_c$  in the  $c$  direction (i.e., about 700 nm) is larger than the film thickness. However, for  $\lambda/\xi \gg 1$  the core pinning (that depends on  $\xi$ ) strongly dominates the magnetic pinning (that depends on  $\lambda$ ).<sup>8</sup> Thus, no pinning effect due to the relatively large penetration depth is expected.

A wide second maximum, extending over a range of  $60^\circ$ , is found for  $\theta = 0^\circ$  and  $180^\circ$  when the flux lines are perpendicular to the film plane [Fig. 1(c)]. Extended two-dimensional defects in line with the  $c$  axis, like twins or stacking faults, act as pinning centers in that case. The twin-boundary distance is about 40 to 80 nm as proved by transmission electron microscopy [Fig. 4(a)]. Also, stacking faults are present in the films as demonstrated in Fig. 4(b).  $j_c$  does not depend on the angle between the normal of these planar pinning centers (i.e., the [110] or [100] direction) and the direction of the flux motion (i.e., the direction of the Lorentz force). This was proved for more than twenty samples where the current paths were randomly oriented with respect to the  $a$  and  $b$  axes. From this it can be concluded that the flux lines cannot glide along these planes or are pinned only at the intersection points. To explain the width of the  $j_c(\theta)$  maximum one can suppose that the current around the vortices tends to flow in the CuO planes.<sup>9</sup> Thus, the

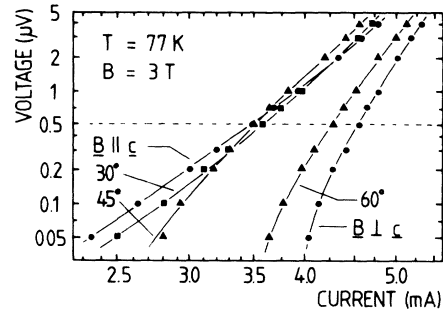


FIG. 5.  $V$ - $I$  curves at 77 K, 3 T, and various field directions in a  $\log V$ - $\log I$  plot. The horizontal dashed line marks the voltage criterion used for the  $j_c$  determination.

flux lines in the sample are still parallel to the  $c$  axis even if the applied magnetic field is tilted by an angle  $\theta$ .

To find out the limits of  $T$ ,  $B$ , and  $\theta$  where strong flux creep can influence the  $j_c$  measurement, some of the  $V$ - $I$  data were analyzed in a  $\log V$ - $\log I$  plot, as discussed by Koch *et al.*<sup>10</sup> For  $T \leq 60$  K all the  $V$ - $I$  curves show a slight negative curvature and flux creep can be excluded if we assume that in the flux-creep region the voltage  $V$  is proportional to  $\sinh I/I_0$ , which always shows positive curvature. However, Griessen<sup>11</sup> reproduced  $\log V$ - $\log I$  curves with negative curvature in a modified flux-creep model, assuming a distribution of the activation energy. For  $T = 77$  K,  $B = 3$  T, and varying the tilt angle, a change of curvature is observed, indicating strong flux creep in the  $\mathbf{B} \parallel \mathbf{c}$  case (see Fig. 5). This change might explain the  $j_c(\theta)$  behavior at 3 T and 77 K which does not fit with the systematics of the data at lower temperatures.

In summary, intrinsic and extrinsic pinning centers determine the critical current density in  $\text{YBa}_2\text{Cu}_3\text{O}_x$  for particular directions of the magnetic field. The effectiveness of the corresponding pinning potentials depends on  $B$  and  $T$ . Evidence for intrinsic pinning between the CuO layers in the  $\mathbf{B} \perp \mathbf{c}$  case and pinning at twin boundaries or stacking faults in the  $\mathbf{B} \parallel \mathbf{c}$  case was found.

The authors thank B. Kabius (Kernforschungsanlage, Jülich) and O. Eibl (Siemens, München) for providing the TEM micrographs, and G. Endres, H. E. Hoenig, K. J. Schmatjko, P. Schmitt, T. Takahashi, and especially B. Hensel for assistance and helpful discussions.

(a) Also at Physikalisches Institut, Universität Erlangen, 8520 Erlangen, West Germany.

<sup>1</sup>T. K. Worthington, W. J. Gallagher, and T. R. Dinger, Phys. Rev. Lett. **59**, 1160 (1987).

<sup>2</sup>B. Roas, L. Schultz, and G. Endres, Appl. Phys. Lett. **53**, 1557 (1988).

<sup>3</sup>B. Roas, L. Schultz, and G. Endres, J. Less-Common Met. **151**, 413 (1989).

<sup>4</sup>M. Tachiki and S. Takahashi, Solid State Commun. **70**, 291 (1989).

<sup>5</sup>G. Saemann-Ischenko, B. Hensel, B. Roas, J. Dengler, G. Ritter, S. Klaumünzer, H. E. Hoenig, H. W. Neumüller, J. Schützmann, M. Franz, W. Ose, K. F. Renk, and D. L. Nagy, *Mod. Phys. Lett. B* (to be published).

<sup>6</sup>V. G. Kogan and L. J. Campbell, *Phys. Rev. Lett.* **62**, 1552 (1989).

<sup>7</sup>A. M. Campbell and J. E. Evetts, *Critical Currents in Superconductors* (Taylor and Francis, London, 1972), pp. 120 and 139.

<sup>8</sup>H. Ullmaier, *Irreversible Properties of Type II Superconductors* (Springer-Verlag, Berlin, 1975), p. 46.

<sup>9</sup>D. E. Farrell, C. M. Williams, S. A. Wolf, N. P. Bansal, and V. G. Kogan, *Phys. Rev. Lett.* **61**, 2805 (1988).

<sup>10</sup>R. H. Koch, V. Foglietti, W. J. Gallagher, G. Koren, A. Gupta, and M. P. A. Fisher, *Phys. Rev. Lett.* **63**, 1511 (1989).

<sup>11</sup>R. Griessen, in *Proceedings of the International Conference on Critical Currents in High  $T_c$  Superconductors*, Karlsruhe, 1989 [Cryogenics (to be published)].

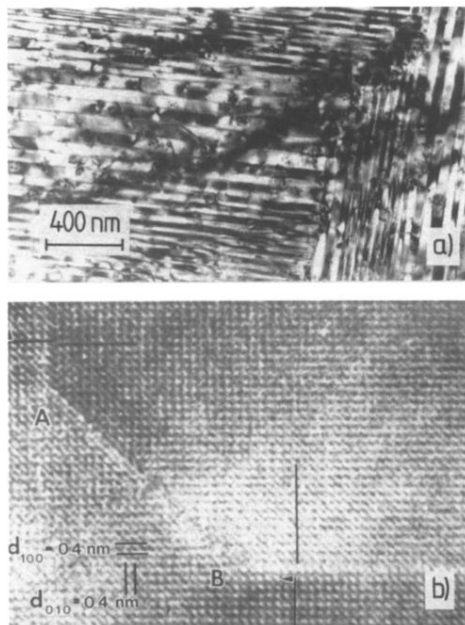


FIG. 4. (a) Twin boundaries along the [110] direction in a laser-deposited  $\text{YBa}_2\text{Cu}_3\text{O}_x$  film. The distance of two boundaries varies from 40 to 80 nm. (b) High-resolution transmission electron micrograph of an epitaxial film in the [001] pole. A stacking fault and a shift of the lattice by half of a unit cell can be seen.